

# Static monitoring of a masonry arch bridge: Evaluating the effects of changing environment

P. Borlenghi & C. Gentile

*DABC, Politecnico di Milano, Milan, Italy*

M. D'Angelo

*DICA, Politecnico di Milano, Milan, Italy*

*Tecnoindagini Srl, Cusano Milanino, Italy*

F. Ballio

*DICA, Politecnico di Milano, Milan, Italy*

**ABSTRACT:** The paper presents selected results obtained in the continuous monitoring of the *Candia* bridge – a historical masonry arch bridge crossing the Sesia River in the north of Italy – to detect scour-induced effects. Generally speaking, hydraulic processes are the main cause of bridge failure, and masonry arch bridges are particularly vulnerable to scour-induced settlements. Consequently, the early detection of anomalies associated to scour is of outmost importance to ensure the safe operation of river bridges. In the present study, measurements of the piers rotation are performed using tiltmeters; in addition, environmental parameters, such as temperature, water level and riverbed changes, are measured to check possible correlation with the monitored rotations. The results from the first two years of monitoring highlight anomalous changes in the rotation-temperature correlation of various piers.

## 1 INTRODUCTION

Masonry bridges with shallow foundations on the riverbed are highly vulnerable to scour-induced settlements. Nevertheless, the number of studies addressing this issue is still limited. Some scholars have tackled the problem with refined numerical models (Zampieri et al. 2017, Tubaldi et al. 2018, Scozzese et al. 2019), limit analysis (George & Menon 2022) or laboratory testing of scaled-down models (Invernizzi et al. 2011). However, extensive studies on the long-term monitoring of scour effects in masonry arch bridges are still missing. The present paper summarizes the results collected in two years of continuous monitoring of the historical multi-span masonry bridge, called *Candia* bridge.

On-site inspections revealed that all pier footings resting on the riverbed underwent strengthening interventions, highlighting the vulnerability to scour actions. In addition, the bridge experienced an intense flood event in October 2020.

The quasi-static monitoring system of the *Candia* bridge was designed to measure the rotations at the top of the piers resting on the riverbed to eventually detect the onset of scour-induced settlement. In more detail, the system includes: (a) 15 MEMS tilt-meters; (b) 1 hydrometer and 1 echo-sounder; (c) 1 weather station; (d) 2 cameras. The tiltmeters measure the traverse rotation of piers at the arches skewback and 2 tilt-meters are installed on the piers that were most affected by the scour events since 2003. In addition, temperature, water level and riverbed variations are monitored by means of thermocouples, hydrometer and echosounder respectively. The system is active since November 2020.

The structure, along with other bridges has been investigated as part of a joint research between Politecnico di Milano and Regione Lombardia aimed at defining guidelines for monitoring key infrastructures (Limongelli et al. 2022) and the subsequent implementation in pilot sensing systems (see, e.g. Bianchi et al. 2022, Borlenghi et al. 2022b, D'Angelo et al. 2022).

After a concise description of the bridge and the Sesia River, the paper focuses on the data collected in the first two years of monitoring.



Figure 1. The *Candia* bridge: view from the upstream of Sesia River.

## 2 THE *CANDIA* BRIDGE: DESCRIPTION AND PRELIMINARY ANALYSIS

The investigated structure (Figure 1) – called *Candia* bridge (Borlenghi et al. 2022a) – is a multi-span masonry arch bridge that crosses the Sesia River between the small municipalities of Candia Lomellina and Casale Monferrato. The structure is 325 m long and it is composed of 16 segmental arches, 15 piers and end abutments. All structural components are built in brick masonry. The arches have a span – measured from the arch skewback – of 17.5 m. As shown in Figure 1, all the piers were subjected to the strengthening of the foundation. The deck width is equal to 10 m and includes a roadway and a railway track, with the latter being inactive since 2010.

### 2.1 *The interaction with the Sesia river*

The structure is located 5 km upstream of the confluence between Sesia River and Po River. The Sesia River has a meandering channel pattern, which appears planimetrically stable from aerial images observation since 1954. In addition, the flow regime of the Sesia River is rather torrential with flow discharges ranging between 70 m<sup>3</sup>/s and 5000 m<sup>3</sup>/s. In case of a 200-year flood event, water can reach an elevation of about 105 m above sea level (asl) and 1 m above the skewback of the bridge arches.

According to Pizarro et al. (2019), scour can be classified as (1) natural scour, (2) contraction scour, and (3) local scour. In case of *Candia* bridge, the natural scour is occurring due to a general degradation of the altimetric profile of the Sesia River: along the period 1960-2000, the river generally eroded for 2-3 m. In addition, local scour at the foundation piers may occur due to local flow turbulences induced by the obstructions in the riverbed: the large concrete plinths reduced the free flow cross-section to 13.5 m. The presence of wood debris can further intensify the local scour process and in the case of *Candia* bridge the presence of important accumulation of debris during floods is well-documented.

Armoring intervention of the riverbed were carried out on several occasions to stabilize the sediments around the foundations. To the authors' knowledge, the last intervention of riverbed stabilization - before the installation of the monitoring system - was performed after 2003 around the most eroded piers at the left side of the channel, where flow concentrates in normal condition. This operation, however, simply modified the local morphology of the riverbed, deviating the main flux - and therefore the scour process - from the left to the central-channel piers. Figure 2 shows a representation of this mechanism.

In October 2020 a serious flood of the Sesia River occurred. The maximum water level reached during the event can be estimated from available photos and it is almost equal to

105 m asl (the quota of the 200-year flood event). The flood caused severe damage to the streets, railway tracks and buildings in areas nearby the bridge. However, no evidence of damage was detected on the bridge. After the flood event, field measurements of water depth were performed with a stadia rod. The local measures on pier P05 – taken from the extrados of the foundation plinth – resulted in 5.5 m at the upstream side and 2.7 m at the downstream side.



Figure 2. Satellite images of the Sesia River before and after the armorment intervention.

## 2.2 Historical and documentary research

Due to the lack of available documentations, an intense historical research was performed to identify the construction period and the main structural interventions.

The bridge was conceivably built between 1868 and 1870. According to the original design drawings – found in a Thesis of the Royal Technical School for Engineers of Turin (Martinengo 1869) – the foundations of the piers were of two types: the piers most subject to the river flow, i.e. those on the river right (P01-P04), were founded at a depth of 2 m below the riverbed (96 m asl), while the remaining ones (P05-P15) were founded 1 m below the riverbed (97 m asl). Surprisingly, at the age of the construction, the main river channel was on the river right.

Between 1954 and 1955 the 9th arch – included among P08 and P09 – was reconstructed and the foundations of piers from P09 to P11 were strengthened a deepening of the foundation level (Figure 3a) up to 12 m below the riverbed. The reason of the heavy damage of the arch is still unknown but most likely it was connected to soil settlements. Subsequently, during the 1980s, a similar intervention on the foundations of piers P04-P08 was performed (Figure 3b), together with the strengthening of arches from 1 to 5.

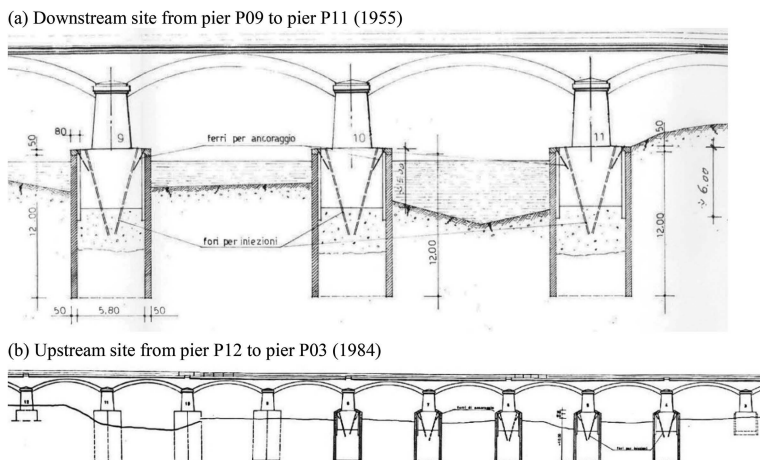


Figure 3. Historical drawings of different strengthening interventions on the piers: (a) 1955 intervention on piers P09, P10 and P11; (b) 1984 intervention on piers from P04 to P08.

To the authors' knowledge and based on the results of the documentary research, the foundation level for piers from P04 to P11 is equal to 12 m (measured from the extrados of the foundation plinth) while the foundation level of piers P01-P03 and P12-P15 is equal to 6 m.

### 3 THE CONTINUOUS MONITORING SYSTEM

The monitoring system installed in the *Candia* bridge (Figure 4a) is composed by: (a) 15 uniaxial MEMS analog tiltmeters (SISGEO model 0S541MA0202, accuracy  $\pm 0.008^\circ$ ); (b) 1 weather station (measuring temperature, humidity, rainfall intensity, wind speed and direction); (c) 1 hydrometer; (d) 1 echo-sounder and (e) 2 cameras.

Figure 4b shows typical installation of one tiltmeter (before the cable connection). The tiltmeters were installed at the skewback of the arches on the upstream side of the bridge, measuring positive transverse rotations along the direction of the river flow. It is worth noting that the pier rotation due to a scour-induced settlement is expected to occur in the opposite direction of the river flow (Tubaldi et al. 2018) and therefore with negative measured rotations. As shown in Figure 4a, the tiltmeters were installed only on the piers located in the riverbed and the piers from P04 to P08 – the ones most affected by the deviation of the main river flux from the left- to the central-channel (Figure 2) – are monitored with two tiltmeters: one for each skewback.

The environmental parameters are measured with the weather station, the hydrometer and the echo-sounder. In addition, the outdoor temperatures are also recorded by the internal thermistor of the tiltmeters. The water level is measured with a hydrometer positioned at the deck level while the evolution of scouring holes is performed with an echo-sounder. As shown in Figure 4c, the echo-sounder is installed on piers 5 at the downstream side: the ideal position of the sensor should be on the upstream side, where the scour hole might develop, however, the intense debris accumulation on the upstream side suggested the installation on the downstream side. The debris accumulation on the piers is detected with 2 cameras taking pictures of the river from the upstream side (Figure 5).

The continuous monitoring system has been active since November 22<sup>nd</sup>, 2020. The sensor network has a sampling frequency of 1 Hz with the only exception of the cameras that acquire pictures every 10 minutes. The recorded data are collected every hour in 1 binary file that is transmitted to Politecnico di Milano for the analysis. In the post-processing phase the recoded data are averaged to obtain a single observation every hour.

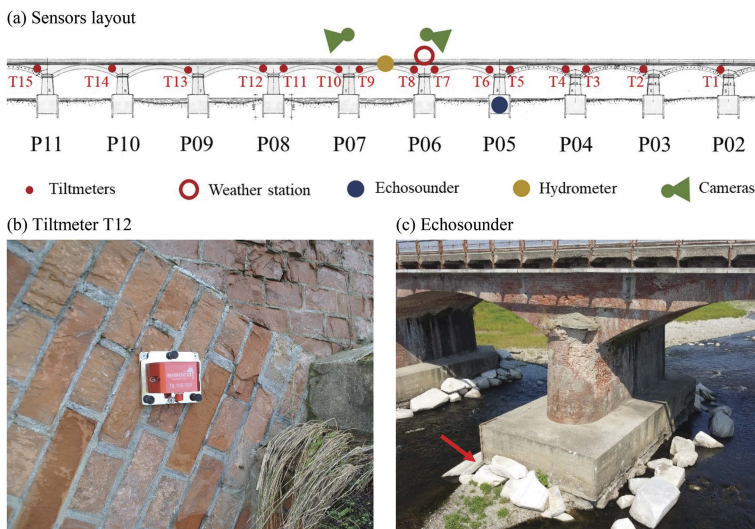


Figure 4. The quasi-static monitoring system: (a) sensors layout; (b) mounting of tiltmeter T12; (c) position of the echosounder.

## 4 DATA ANALYSIS

This section summarises the main results of the quasi-static monitoring system for a period of 2 years, from 31/12/2020 to 01/01/2023. During this time period 16,510 1-h dataset were collected and analysed together with the upstream side pictures taken with the permanent cameras in the daylight (e.g. Figure 5).

Firstly, the main environmental parameters, i.e. outdoor temperature and water level, are processed. Figure 6a illustrates the evolution of the outdoor temperature measured from the internal thermistor of one tiltmeter. The maximum and minimum recorded temperatures in the selected period are equal to 45.7°C and -7.3°C, respectively. However, the temperatures below -1.2°C were ignored in the present paper due to an occasional sensor malfunctioning.

Figure 6b presents the time evolution of the river water level measured with the hydrometer in terms of elevation above sea level (m asl). The average recorded value in the selected period is 97.0 m asl while the maximum value is equal to 100.6 m asl (12 May 2021). It is worth considering that during the expected 200-year event, the river water level can reach an elevation of about 105 m asl, namely, rising about 8 m from the average water level. In the selected period the maximum detected rising is about 3.6 m from the average water level.

Regarding the analysis of debris accumulation Figure 5a shows the important wood debris accumulated over the concrete foundation basement of pier P05 after the flooding of October 2020 (estimated water level reach during the event equal to 105 m asl). After six months an event with a water level of 100 m asl occurred in May 2021 and a substantial variation in the debris accumulation is visible from Figure 5b.



Figure 5. Pictures from the permanently installed cameras: (a) debris accumulation on P05 in November 2020 resulting from the important event of October 2020; (b) debris accumulation on P05 and P04 after the event of May 2021.

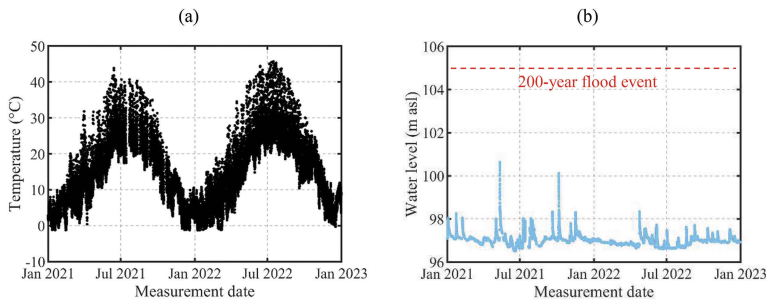


Figure 6. Time evolution of environmental parameters: (a) measured temperature and (b) water level.

Due to the limited length of the present paper only the results of the four most representative tiltmeters are reported: T3, T4, T7 and T8. The selected sensors belong to piers P04 and P06, namely two of the piers most affected by the deviation of the main river flux from the left-

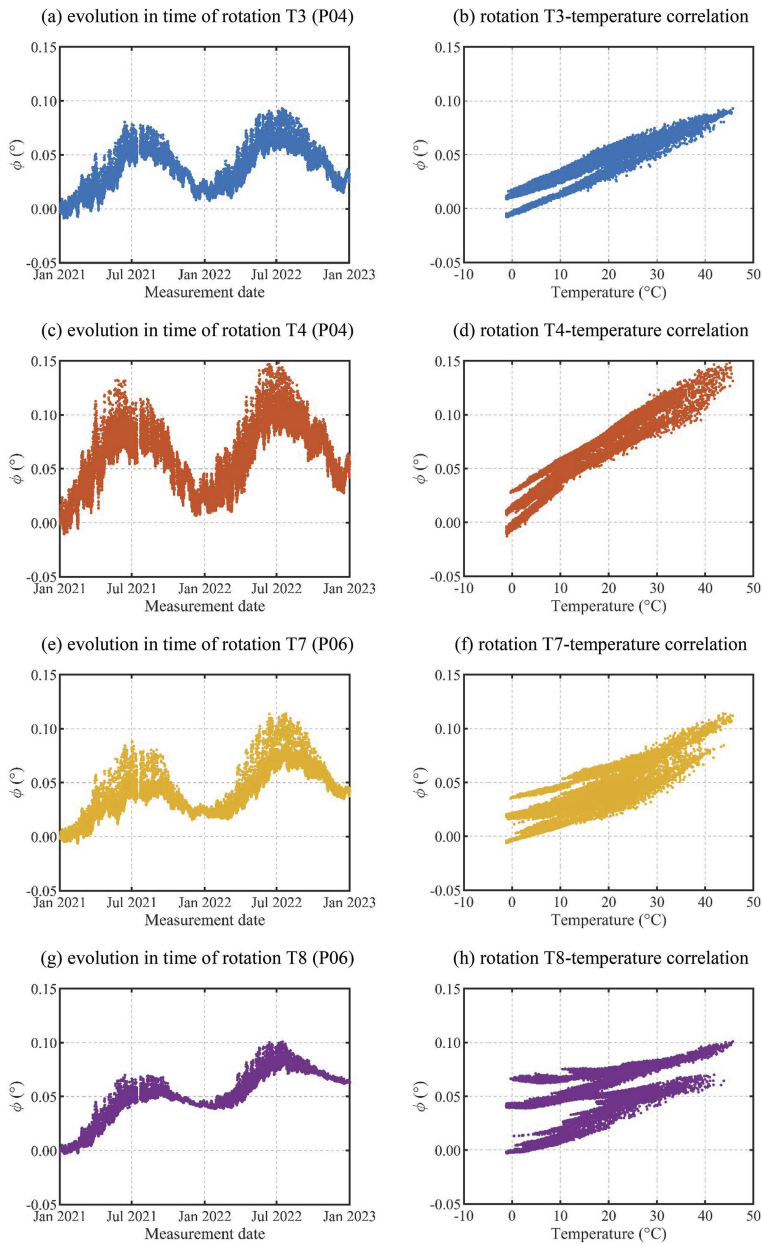


Figure 7. Time variation of rotations and rotation-temperature correlation of sensors T3 (P04), T4 (P04), T7 (P06) and T8 (P06).

Table 1. Statistics of the measured rotations from January 1<sup>st</sup> 2021 to January 1<sup>st</sup> 2023.

Tiltmeter	$\phi_{ave}$ (°)	$\phi_{min}$ (°)	$\phi_{max}$ (°)	$\sigma_x$ (°)	CV (%)
T3	0.036	-0.008	0.093	0.020	56.0
T4	0.060	-0.013	0.148	0.030	50.5
T7	0.039	-0.006	0.114	0.022	57.0
T8	0.050	-0.003	0.101	0.023	46.6

the central-channel after 2003 (Figure 2). Table 1 reports the statistical analysis of the measured rotations.  $\varphi_{ave}$ ,  $\varphi_{min}$  and  $\varphi_{max}$  denotes the average, minimum and maximum values of recorded respectively;  $\sigma_x$  represents the standard deviation and CV the coefficient of variation. The maximum daily variation – experienced during the summer – ranges between  $\pm 0.028^\circ$  for T8 and  $\pm 0.075^\circ$  for T4, while the seasonal variations are about two times larger, ranging from  $\pm 0.06^\circ$  for T8 and  $\pm 0.14^\circ$  for T4.

Firstly, the qualitative comparison of Figures 7a, c, e, g and Figure 6a suggest that the fluctuations of the measured pier rotations approximately follow the temperature variations with a direct correlation: the rotations increase with the increase of temperature. However, the inspection of the time evolution of measured rotations (Figure 7a, c, e, g) reveals that between January 2021 and January 2023 – periods in which temperatures are similar – there is a clear accumulation of rotation, ranging from  $+0.02^\circ$  for T3 to  $+0.06^\circ$  for T8. In addition, as shown in Figures 7b, d, f, h, the rotation-temperature correlation exhibits various changes during the monitoring period, highlighting the presence of different anomalies.

Tubaldi et al. 2018 analyzed scour effects on a two-span masonry bridge with a novel modelling procedure. The research highlight that: (a) the effects of scouring-induced settlements are related with pier-foundation rotations in the opposite direction of the river flow; (b) the pier displacements start to increase beyond the values induced by vertical loads only after the maximum scour depth exceeds the foundation depth. The previous considerations can be related to the present work as follow:

- The tiltmeters of *Candia* bridge experienced an accumulation of rotation in the direction of the river flow; therefore, the phenomenon that caused the residual rotations should be related to a soil settlement of the downstream side. It is worth considering that the distribution of vertical loads is not symmetric: the railway track – decommissioned in 2010 – is on the upstream side while the roadway is on the downstream side, causing an asymmetric distribution of service loads.
- According to the blueprints of the different interventions (Figure 3) the foundations depth for all the piers should be equal to approximately 12 m (measured from the extrados of the foundation plinth). During an onsite survey a local measure of the scour hole depth on the upstream side of pier P05 was equal to 5.5 m. Consequently, the system should record the negative rotation residuals only if new important hydraulic events will occur.

## 5 CONCLUSIONS

The paper illustrates the first two years of results from the continuous monitoring system recently designed and installed on the historical masonry arch bridge of *Candia* over the Sesia River.

The main aim of the monitoring system is to detect scour-induced pier settlements. Variations in the structural behavior of the bridge are measured with a series of MEMS tiltmeters installed on top of the bridge piers. To account for the hydraulic actions, and for the scour in particular, a hydrometer, an echo-sounder, and two cameras were installed. It is worth noting that relevant flood events – which would induce scour – did not occur during the first two years of recording. Due to the limited length of the paper, only four tiltmeters are analyzed in the presented research (i.e. T3, T4, T7 and T8).

From the analysis of the recorded data, the following conclusions can be drawn:

- The tilt variations in the considered monitoring period range from  $-0.013^\circ$  to  $+0.148^\circ$ .
- The outdoor temperature is confirmed as the dominant driver for the tilt variations; however, the rotation-temperature correlation changes different times during the monitoring period.
- Between January 2021 and January 2023 there is a clear accumulation of rotation, ranging from  $+0.02^\circ$  for T3 to  $+0.06^\circ$  for T8.
- The water elevation does not show any correlation with the pier rotations. However, the recorded water level variations are negligible in respect to the flood events experienced by the structure in October 2020, before the monitoring system installation.

The physical phenomenon that caused the identified permanent shifts in the rotation- temperature correlation is still not clear. To this purpose onsite visual inspections are periodically performed to detect the onset of possible cracks in the arches. However, it is worth considering that the detected anomalies are not directly correlated with scour-induced settlements: the scour action induces a rotational mechanism at the base of the piers on the upstream side, while the identified permanent rotations occurred (most likely) due to settlements in the downstream side.

Within the following months, new investigations are planned using drones, laser-scanner surveys and local measures of scour hole depth at central pier foundations.

## ACKNOWLEDGEMENTS

The support of Regione Lombardia is gratefully acknowledged. Sincere thanks are due to G. Cazzulani, PhD (MECC, Politecnico di Milano), G. Zonno, PhD (DABC, Politecnico di Milano), M. Cucchi and M. Iscandri (LPMSC, Politecnico di Milano) who assisted the authors during the installation of the monitoring system.

## REFERENCES

- Bianchi, S., Biondini, F., Rosati, G., Anghileri, M., Capacci, M., Cazzulani, G. & Benedetti, L. 2022. Structural Health Monitoring of Two Road Bridges in Como, Italy. In Pellegrino, C., *et al.* (eds) *Proceedings of the 1st Conference of the European Association on Quality Control of Bridges and Structures, EUROSTRUCT 2021; Padua*, 29 August - 1 September 2021. Lecture Notes in Civil Engineering, vol 200. Springer, Cham.
- Borlenghi, P., D'Angelo, M., Ballio, F. & Gentile, C. 2022. Continuous Monitoring of Masonry Arch Bridges to Evaluate the Scour Action. In Pellegrino, C., *et al.* (eds) *Proceedings of the 1st Conference of the European Association on Quality Control of Bridges and Structures, EUROSTRUCT 2021; Padua*, 29 August - 1 September 2021. Lecture Notes in Civil Engineering, vol 200. Springer, Cham.
- Borlenghi, P., Gentile, C. & Zonno, G. 2022. Monitoring Reinforced Concrete Arch Bridges with Operational Modal Analysis. In Pellegrino, C., *et al.* (eds) *Proceedings of the 1st Conference of the European Association on Quality Control of Bridges and Structures, EUROSTRUCT 2021; Padua*, 29 August - 1 September 2021. Lecture Notes in Civil Engineering, vol 200. Springer, Cham.
- D'angelo, M., Menghini, A., Borlenghi, P., Bernardini, L., Benedetti, L., Ballio, F., Belloli, M. & Gentile, C. 2022. Hydraulic Safety Evaluation and Dynamic Investigations of Baghetto Bridge in Italy. *Infrastructures* 7(4): 53.
- George, J. & Menon, A. 2022. Kinematic approach for scour analysis of masonry arch bridges. *Engineering Failure Analysis* 141:106703.
- Invernizzi, S., Lacidogna, G., Manuello, A. & Carpinteri, A. 2011. AE monitoring and numerical simulation of a two-span model masonry arch bridge subjected to pier scour. *Strain* 47(SUPPL. 2):158–169
- Limongelli, M.P., Gentile, C., Biondini, F., di Prisco, M., Ballio, F., Zonno, G., Borlenghi, P., Bianchi, S., Capacci, L., Anghileri, M., Zani, G., Scalbi, A., Ferreira, K.F., D'Angelo, M., Cazzulani, G., Benedetti, L., Somaschini, C., Bernardini, L., Belloli, M., Resta, F., Vigo, P. & Colombo, A. 2022. Bridge structural monitoring: the Lombardia regional guidelines. *Structure and Infrastructure Engineering*: article in press.
- Martinengo, L. 1869. *Ponte in muratura sul fiume Sesia nella ferrovia in costruzione di Asti-Casale-Mortara*. Regia Scuola d'Applicazione per gli Ingegneri di Torino.
- Pizarro, A., Manfreda, S. & Tubaldi, E. 2020. The science behind scour at bridge foundations: A review. *Water* 12(2):374.
- Scozzese, F., Ragni, L., Tubaldi, E. & Gara, F. 2019 Modal properties variation and collapse assessment of masonry arch bridges under scour action. *Engineering Structures* 199:109665.
- Tubaldi, E., Macorini, L. & Izzuddin, B.A. 2018. Three-dimensional mesoscale modelling of multi-span masonry arch bridges subjected to scour. *Engineering Structures* 165: 486–500.
- Zampieri, P., Zanini, M.A., Faleschini, F., Hofer, L. & Pellegrino, C. 2017. Failure analysis of masonry arch bridges subject to local pier scour. *Engineering Failure Analysis* 79:371–384.